The Effect of Spanwise-Varying Impedance on Acoustic Liner Impedance Eduction

Lucas A. Bonomo*, Júlio A. Cordioli†,
Federal University of Santa Catarina, 88040-900 Florianópolis, Brazil

Edward J. Brambley‡,
University of Warwick, Coventry CV4 7AL, United Kingdom

Francesco Avallone§
Politecnico di Torino, 10129, Torino, Italy

I. Introduction

Acoustic liners are commonly modeled through a locally reacting acoustic impedance, a frequency-dependent complex quantity that depends on liner geometry and operating conditions such as grazing-flow velocity, flow profile, and sound pressure level [1–4]. Under grazing flow, impedance eduction is the standard experimental approach for liner characterization, since it infers the liner impedance from in-duct acoustic measurements and a duct propagation model [5–8].

In many impedance-eduction studies, the lined wall is effectively treated as uniform in the spanwise direction. In our recent study, Ref. [9], we investigated the role of realistic sheared flow profiles on acoustic propagation and impedance eduction in rectangular ducts, showing that simplified propagation models can remain accurate provided the effective mean flow is treated consistently, i.e., if realistic formulations for the boundary layer are used when shear flow is assumed. However, the acoustic impedance of liners is known to depend on the local grazing-flow conditions over the facesheet [4]. Since dedicated liner test rigs usually employ rectangular ducts, with small aspect ratio, the flow profile is inherently three-dimensional, suggesting that the liner impedance may vary spatially across the span of the sample. The present work therefore examines whether the usual uniform impedance assumption remains adequate when the local flow profile induces spanwise variations in liner impedance. A numerical experiment is performed in which axial wavenumbers are synthesized for a lined duct with sheared flow and variable wall impedance, and then compared with the results obtained when the same liner is represented by its spanwise-averaged impedance. The impact of this simplification on impedance eduction is then assessed using the traditional straightforward method [6].

*Postdoctoral Research Fellow, Laboratory of Vibration and Acoustics, lucas.bonomo@lva.ufsc.br, AIAA Member.
†Associate Professor, Department of Mechanical Engineering, julio.cordioli@ufsc.br, AIAA Member.
‡Reader (Associate Professor), Warwick Mathematics Institute and WMG, E.J.Brambley@warwick.ac.uk, AIAA Senior Member.
§Full Professor, Department of Mechanical and Aerospace Engineering, francesco.avallone@polito.it, AIAA Member.

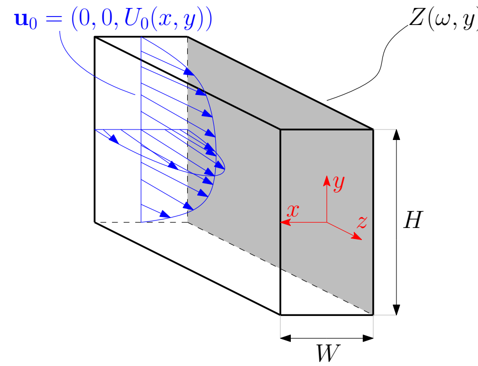

Fig. 1 The duct geometry and coordinate system used here.

II. Problem Description

For the present study, the infinite rectangular duct shown in Fig. 1 is considered. The duct has width W and height H, with an axial mean flow profile $\boldsymbol{u}_0 = U_0(x, y)\boldsymbol{e}_z$. In contrast with our previous study, where the lined wall was modeled with a spanwise uniform impedance, in this work we assume a locally reacting impedance that varies in the spanwise direction, $Z(\omega, y)$, along the lined wall at $x = -W/2$. All other walls are acoustically rigid.

A. Governing formulation

Following the formulation presented in Ref. [9], the acoustic field is modeled using the 3D-Pridmore–Brown equation, assuming axial invariance and harmonic dependence in time and in the axial direction. The resulting problem is discretized as a generalized eigenvalue problem using a pseudo-spectral Chebyshev collocation approach, the numerical solution of which is as described in Ref. [9]. For reference, comparisons are also made with the uniform-flow model based on the Convected Helmholtz Equation and the Ingard–Myers boundary condition.

B. Flow profile

In this work, the mean flow is represented by the tensorized law-of-the-wall profile. The one-dimensional profile is based on the Van Driest formulation [10], with a smooth correction introduced to enforce zero derivative at the duct centerline, and is shown in Fig. 2. The resulting midspan profiles in the x and y directions are then tensorized and rescaled by the bulk Mach number, yielding

$$\frac{U_0(x, y)}{c_0} = M \frac{U_x(x)}{\langle U_x(x) \rangle} \frac{U_y(y)}{\langle U_y(y) \rangle}, \tag{1}$$

where $\langle \cdot \rangle$ denotes averaging over the corresponding one-dimensional domain. The bulk Mach number is given by

$$M = \frac{1}{WH} \int_{-W/2}^{W/2} \int_{-H/2}^{H/2} \frac{U_0(x, y)}{c_0} \mathrm{d}y \mathrm{d}x. \tag{2}$$

Additional details on the profile construction are omitted here for brevity and can be found in Ref. [9].

C. Impedance model

The spatial dependence of the impedance is the key element of this study. The liner impedance is modeled using the Goodrich

(UTAS) model [11],

$$Z(\omega, y) = R(\omega) + R_{\mathrm{cm}}(y) + \mathrm{i}X(\omega), \tag{3}$$

where $R(\omega)$ and $X(\omega)$ are the static (no flow) resistance and reactance, respectively, and $R_{\mathrm{cm}}(y)$ is the grazing-flow-induced resistance term. Note that, in this model, the reactance is assumed uniform over the lined wall. For this case,

$$R_{\mathrm{cm,UTAS}}(y) = \frac{M_{\mathrm{1D}}(y)}{\sigma\left(2 + 1.256\dfrac{\delta^*_{\mathrm{1D}}(y)}{d}\right)}, \tag{4}$$

where σ is the open-area ratio, d is the perforation diameter, and $M_{\mathrm{1D}}(y)$ and $\delta^*_{\mathrm{1D}}(y)$ are the flow Mach number and boundary layer displacement thickness (BLDT) evaluated at this liner location y,

$$M_{\mathrm{1D}}(y) = \frac{1}{W}\int_{-W/2}^{W/2} \frac{U_0(x, y)}{c_0}\mathrm{d}x, \tag{5a}$$

$$\delta^*_{\mathrm{1D}}(y) = \int_{-W/2}^{0} \frac{U_0(x, y)}{U_0(x = 0, y)}\mathrm{d}x. \tag{5b}$$

A demonstration of the slicing procedure used to obtain M_{1D} and δ^*_{1D} is shown in Fig. 2.

The liner geometry is taken from the scanned sample reported by Ref. [12], representative of a typical Single-Degree-Of-Freedom (SDOF) liner, with perforation diameter 1.17 mm, facesheet thickness 0.55 mm, open-area ratio of approximately 8.8 %, and cavity depth of 38.1 mm.

In addition to the reference distribution $R_{\mathrm{cm,UTAS}}(y)$, two idealized spanwise distributions are considered in order to assess the effects of larger impedance variation across the liner while preserving the same spatial average. These are given by

$$R_{\mathrm{cm,linear}}(y) = 2\left\langle R_{\mathrm{cm,UTAS}}(y)\right\rangle \left[1 - \frac{2|y|}{H}\right], \quad \text{and} \tag{6a}$$

$$R_{\mathrm{cm,parabolic}}(y) = 1.5\left\langle R_{\mathrm{cm,UTAS}}(y)\right\rangle \left[1 - \left(\frac{2y}{H}\right)^2\right]. \tag{6b}$$

The resulting reference impedances are shown in Fig. 3. For the parameters considered here, most of the liner resistance is associated with the flow-dependent term R_{cm}, whereas the contribution of the static term $R(\omega)$ is small.

D. Numerical synthesized experiment

The numerical framework described above is used to perform two *in silico* experiments. First, the Pridmore-Brown eigenvalue solver is used to compute the axial wavenumbers $k_z^{\pm}(Z(\omega, y))$ of the least-attenuated mode with the spanwise-varying impedance $Z(\omega, y)$. These synthetic data are compared against the wavenumbers $k_z^{\pm}(\langle Z(\omega, y)\rangle)$ obtained using the same flow but with a uniform impedance equal to the spanwise average of the original distribution, $\langle Z(\omega, y)\rangle$. Here, the superscripts + and − denote downstream- and upstream-propagating modes, respectively. The objective of this numerical experiment is therefore to assess the error in the predicted wave propagation behaviour introduced when a spanwise-varying impedance distribution is replaced by its average value.

Secondly, the synthetic data $k_z^{\pm}(Z(\omega, y))$ with the spanwise-varying impedance $Z(\omega, y)$ are used as input to an impedance eduction calculation to educe a spanwise-constant impedance $Z_{\mathrm{edu}}(\omega)$. In effect, these wavenumbers are *in silico* analogs of experimental wavenumbers identified from in-duct pressure measurements using Prony-like methods. Based on the findings of Ref. [9], and for the sake of conciseness, the analysis is restricted to the traditional straightforward eduction method, using the bulk Mach number M together with the Ingard–Myers boundary condition. This experiment provides an estimate of the error introduced when a traditional eduction routine assumes a uniform wall impedance.

The mean flow profile, duct geometry, and numerical settings are the same as those adopted in our previous study Ref. [9]. In particular, the calculations are performed for a rectangular duct with $W = 40$ mm and $H = 100$ mm, bulk Mach number $M = 0.3$, frequencies from 500 Hz to 3000 Hz in 100 Hz increments, and friction velocities $u_{\tau,x} = 3.95\,\mathrm{m\,s^{-1}}$ and $u_{\tau,y} = 3.71\,\mathrm{m\,s^{-1}}$.

III. Results and Discussion

A. Wavenumbers

Figure 4 compares the axial wavenumbers of the least-attenuated mode for the four impedance distributions considered in this work. Panels (a,c) show the real part and panels (b,d) the imaginary part of the wavenumbers for downstream (k_z^+) and upstream propagation (k_z^-) (upstream and downstream acoustic sources, respectively). For reference, the solution obtained assuming uniform flow, the IMBC, and the averaged impedance are also shown.

Good agreement is observed between the sheared-flow solution obtained with the averaged impedance and the corresponding IMBC result, consistent with our previous findings [9]. The same behavior is observed for the spanwise-varying impedance using the UTAS-based distribution, whose wavenumbers remain close to those obtained for the averaged impedance. This indicates that, for the conditions considered here, the spanwise variation naturally induced by a realistic high-Reynolds-number turbulent boundary layer flow profile has only a limited effect on the least-attenuated mode.

In contrast, the idealized linear and parabolic distributions lead to larger deviations from the averaged-impedance result, especially near the liner resonance. In these cases, the imaginary part of the axial wavenumber shows a marked increase in magnitude, indicating stronger attenuation. These results suggest that replacing $Z(\omega, y)$ by its spanwise average is adequate for mild impedance variations, but may become inaccurate when stronger spanwise variations are present.

It is also worth noting that the relevant parameter controlling the sensitivity to the local boundary-layer displacement thickness is δ^*/d, rather than δ^* alone. Since this ratio appears in the denominator of the Goodrich model, Eq. (4), the effect of spanwise variations in δ^* is expected to increase for liners with smaller perforation diameters.

B. Simulated impedance eduction

The impedances educed from the wavenumbers obtained with the PBE solver for both the spatially varying and the averaged-impedance cases are shown in Fig. 5. Good agreement is observed between the educed reactances and the reference value, suggesting that reactance eduction is not significantly affected by the presence of a variable resistance. In contrast, the educed resistances for the linear and parabolic impedance distributions diverge notably from

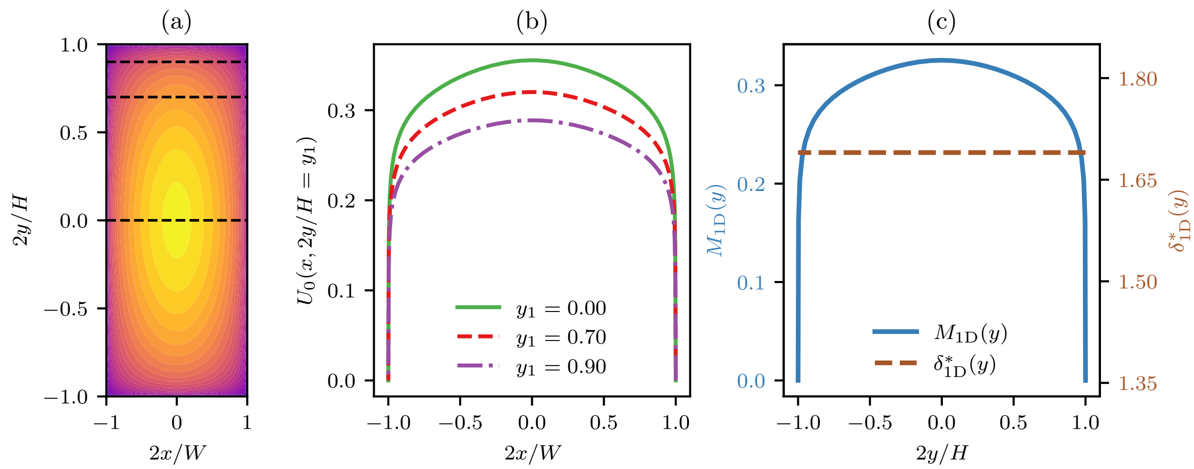

Fig. 2 The 2D axial velocity $U_0(x, y)$ (a), 1D slices at various spanwise locations (b), and the corresponding local flow parameters $M_{1D}(y)$ and $\delta^*_{1D}(y)$ (c).

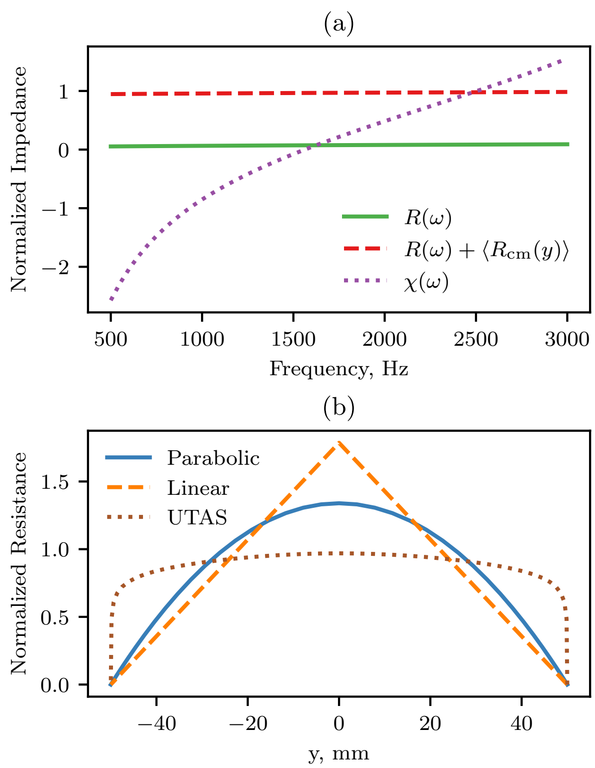

Fig. 3 The various impedance models used here: (a) variation of average values with frequency; (b) spanwise variation.

the averaged impedance, with visible discrepancies between propagation directions. This indicates that large transverse impedance variation may affect impedance-eduction results, although the observed trend does not resemble the classical upstream/downstream discrepancy typically reported in the literature [e.g. 13].

On the other hand, the impedances educed from the wavenumbers corresponding to the averaged impedance and the UTAS-like spatial variation agree well with the reference for both propagation directions. This suggests that, for realistic spatial variations, the assumption of a uniform impedance may still yield accurate results in impedance eduction.

IV. Conclusion

This work investigated the effects on wave propagation and impedance eduction of a liner impedance that varies in the spanwise direction; for example, due to the local sheared grazing-flow profile. A numerical experiment was used to compare the acoustic wavenumbers and educed impedances obtained for spanwise-varying impedance distributions with those obtained when the same liner is represented by its averaged impedance.

For the physically inspired impedance variation based on the Goodrich model, both the wavenumbers and the educed impedance remained close to those obtained for the averaged-impedance case. In contrast, the idealized linear and parabolic impedance distributions, which impose larger spanwise variations than the physically inspired case, produced noticeable deviations, especially in the educed resistance near the liner resonance. These results suggest that the assumption of a uniform wall impedance remains adequate for realistic spanwise variations of the type expected in rectangular liner test rigs, but may become inaccurate when stronger transverse variations are present.

The present results are most directly relevant to the rectangular ducts used in laboratory tests, where the grazing-flow profile is inherently nonuniform across the liner. Future work could address more general local-impedance models, including combined effects of spanswise varying grazing flow and SPL, as well as configurations with cylindrical or other duct geometries or axial variations in flow or SPL.

Acknowledgments

J.A. Cordioli acknowledges funding from CNPq (National Council for Scientific and Technological Development). L.A. Bonomo acknowledges funding from the Coordenação de Aperfeiçoamento de Pessoal de Nível Superior – Brasil (CAPES), Finance Code 001. E.J. Brambley acknowledges funding from the UK Engineering and Physical Sciences Research Council (EPSRC grant EP/V002929/1). F. Avallone is co-funded by the European Union (ERC, LINING,

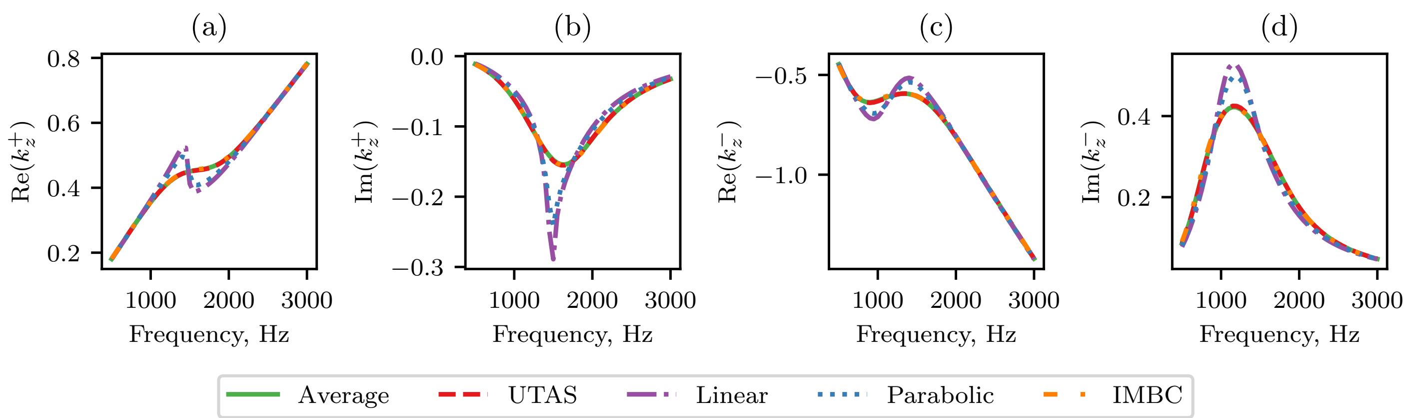

Fig. 4 Real and imaginary parts of the axial wavenumbers for the four impedance distributions and the IMBC solution.

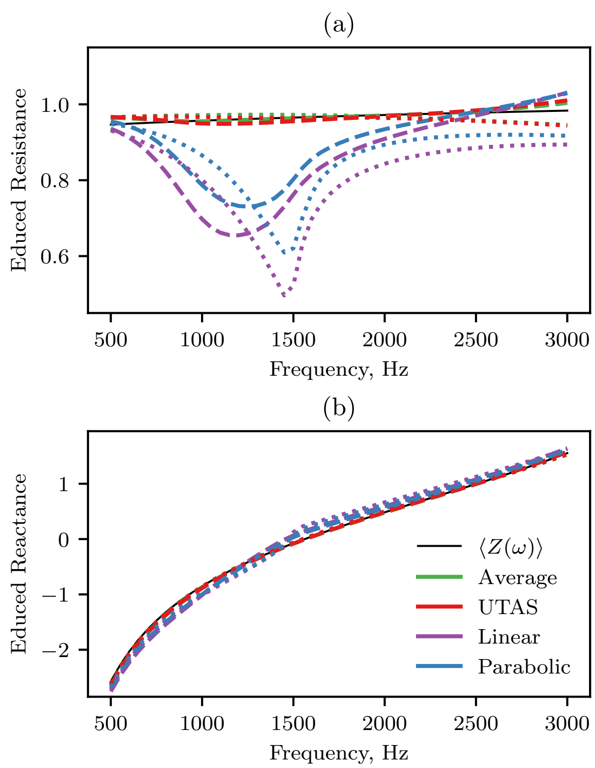

Fig. 5 Educed resistances and reactances for different impedance variations. Dashed lines are educed from upstream-propagating modes (k_z^-). Dotted lines are educed from downstream-propagating modes (k_z^+).

101075903). Views and opinions expressed are however those of the authors only and do not necessarily reflect those of the European Union or the European Research Council Executive Agency. Neither the European Union nor the granting authority can be held responsible for them. Funding is acknowledged from the AeroAcoustics Research Consortium (AARC); the AARC is a government-industry partnership supporting pre-competitive research for aircraft noise reduction. For the purpose of open access, the authors have applied a Creative Commons Attribution (CC BY) licence to any Author Accepted Manuscript version arising from this submission.

References

[1] Guess, A. W., "Calculation of Perforated Plate Liner Parameters from Specified Acoustic Resistance and Reactance," *Journal of Sound and Vibration*, Vol. 40, No. 1, 1975, pp. 119–137. https://doi.org/10.1016/S0022-460X(75)80234-3.

[2] Jones, M., Tracy, M., Watson, W., and Parrott, T., "Effects of Liner Geometry on Acoustic Impedance," *8th AIAA/CEAS Aeroacoustics Conference*, AIAA, 2002, p. 2446. https://doi.org/10.2514/6.2002-2446.

[3] Murray, P., and Astley, R. J., "Development of a Single Degree of Freedom Perforate Impedance Model under Grazing Flow and High SPL," *18th AIAA/CEAS Aeroacoustics Conference*, AIAA, 2012, p. 2294. https://doi.org/10.2514/6.2012-2294.

[4] Kooi, J., and Sarin, S., "An Experimental Study of the Acoustic Impedance of Helmholtz Resonator Arrays under a Turbulent Boundary Layer," *7th Aeroacoustics Conference*, AIAA, 1981, p. 1998. https://doi.org/10.2514/6.1981-1998.

[5] Watson, W., Jones, M., and Parrott, T., "Validation of an Impedance Eduction Method in Flow," *AIAA Journal*, Vol. 37, No. 7, 1999, pp. 818–824. https://doi.org/10.2514/2.7529.

[6] Jing, X., Peng, S., and Sun, X., "A Straightforward Method for Wall Impedance Eduction in a Flow Duct," *The Journal of the Acoustical Society of America*, Vol. 124, No. 1, 2008, pp. 227–234. https://doi.org/10.1121/1.2932256.

[7] Elnady, T., Bodén, H., and Elhadidi, B., "Validation of an Inverse Semi-Analytical Technique to Educe Liner Impedance," *AIAA Journal*, Vol. 47, No. 12, 2009, pp. 2836–2844. https://doi.org/10.2514/1.41647.

[8] Bonomo, L. A., Quintino, N. T., Spillere, A., Cordioli, J. A., and Murray, P. B., "A Comparison of In-Situ and Impedance Eduction Experimental Techniques for Acoustic Liners with Grazing Flow and High SPL," *28th AIAA/CEAS Aeroacoustics Conference*, AIAA, 2022, p. 2998. https://doi.org/10.2514/6.2022-2998.

[9] Bonomo, L. A., Cordioli, J. A., Brambley, E. J., Paudano, A., and Avallone, F., "Sheared flow profile effects on acoustic impedance eduction in small 3D ducts," *arxiv*, 2025. https://doi.org/https://doi.org/10.48550/arXiv.2511.1937, Preprint submitted to AIAA Journal.

[10] Van Driest, E. R., "On turbulent flow near a wall," *Journal of the aeronautical sciences*, Vol. 23, No. 11, 1956, pp. 1007–1011. https://doi.org/10.2514/8.3713.

[11] Yu, J., Ruiz, M., and Kwan, H. W., "Validation of Goodrich Perforate Liner Impedance Model Using NASA Langley Test Data," *14th AIAA/CEAS Aeroacoustics Conference*, 2008, p. 2930. https://doi.org/10.2514/6.2008-2930.

[12] Quintino, N. T., Bonomo, L. A., Cordioli, J. A., Jones, M. G., Howerton, B. M., Nark, D. M., and Avallone, F., "Comparison of Impedance Eduction Test Rigs with Different Boundary-Layer Profiles," *AIAA Journal*, Vol. 63, No. 11, 2025, pp. 4872–4883. https://doi.org/10.2514/1.J065173.

[13] Renou, Y., and Aurégan, Y., "Failure of the Ingard–Myers Boundary Condition for a Lined Duct: An Experimental Investigation," *The Journal of the Acoustical Society of America*, Vol. 130, No. 1, 2011, p. 52. https://doi.org/10.1121/1.3586789.